Live Cell Imaging

DOI: 10.1002/anie.201103273

Bioorthogonal Probes for Polo-like Kinase 1 Imaging and Quantification**

*Ghyslain Budin, Katherine S. Yang, Thomas Reiner, and Ralph Weissleder**

Polo-like kinase 1 (PLK1) is a critical mediator of the cell cycle, regulating mitotic progression. Specific functions of PLK1 during mitosis include chromosome segregation, centrosome maturation, bipolar spindle formation, regulation of the anaphase-promoting complex/cyclosome (APC/C), coordination of cytokinesis, and regulation of the DNA damage checkpoint.[1–3] This serine/threonine kinase also plays an essential role in mitotic entry by promoting Cdk1-cyclin B activation and nuclear translocation through phosphorylation of Cdc25C,[4,5] Wee1,[6] Myt1,[7] and cyclin B.[8,9] PLK1 consists of two domains, an N-terminal catalytic serine/threonine kinase domain and a C-terminal polo-box domain (PBD).[3] The PBD recognizes specific phosphorylated targeting sequences that are essential for interaction of PLK1 with its substrates and for PLK1 localization to centrosomes, spindles, kinetochores, and the midzone/midbody during mitosis.[10–13]

Given the role of PLK1 in mitotic progression it is perhaps not surprising that overexpression has been shown to lead to oncogenic transformation.[14] Increased PLK1 levels have been found in a wide variety of cancers, including breast, lung, colorectal, ovarian, pancreatic, prostate and head and neck cancers.[15] Since PLK1 expression correlates with cell proliferation, it has been suggested as an early marker for cancer detection, as well as a prognostic marker.[16] However, to date it has been difficult to visualize and quantify PLK1 expression directly in patient samples or in live cells due to the lack of imaging agents available for intracellular/nuclear targets such as PLK1. Having the ability to monitor PLK1 directly in live cells or by whole body imaging (where cells cannot be fixed and antibodies do not reach nuclear targets) would have far reaching applications in the development of future PLK1 inhibitors and for a better understanding of its biology.

Among the available small-molecule inhibitors targeting PLK1, BI 2536 is currently the most intensively studied and potent inhibitor in clinical trials (Figure 1 A).[17,18] BI 2536 binds to and inhibits PLK1, leading to mitotic arrest, disruption of cytokinesis, and apoptosis.[18] BI 2536 exhibits over 10000-fold selectivity towards PLK1 as compared to 63 other kinases and only minimal activity against the closely related kinases PLK2 and PLK3.[17,18] BI 2536 has been tested on numerous human cancer cell lines in vitro, and confirmed in xenograft models showing prominent anti-cancer activity.[18]

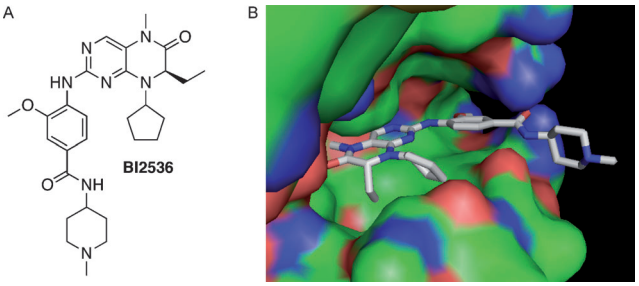

Figure 1. A) Chemical structure of BI 2536; B) Crystal structure of PLK1 in complex with BI 2536 (PDB ID: 2RKU).[20]

Based on the implications of PLK1 in human tumors, the clinical development of PLK1 inhibitors and the inability to visualize the target readily in vivo, we sought to develop small-molecule PLK1 imaging agents based on BI 2536 scaffold, using a modular bioorthogonal approach. Specifically, we modified a BI 2536 precursor with *trans*-cyclooctene (TCO) which can then react bioorthogonally with tetrazine (Tz) moieties to rapidly test and develop lead candidates into optical or isotope based imaging agents.[19] Here we report the first use of BI 2536-TCO as an imaging agent for PLK1 in live cells and as a tool to quantify protein expression levels.

The crystal structure of PLK1 in complex with BI 2536 (PDB ID 2RKU)[20] shows that the *N*-methylpiperazine residue does not participate in ligand–protein interaction and is oriented towards the solvent (Figure 1 B). Based on the crystal structure of PLK1 and BI 2536, we reasoned that a modification on the aromatic carboxylic acid of BI 2536 should not majorly affect the affinity of the drug for PLK1.

BI 2536-TCO was synthesized in eight steps with an overall yield of 4% (Scheme 1).[21] Briefly, esterification of the commercially available D-2-aminobutyric acid followed by a reductive amination with cyclopentanone afforded compound **2** in 97% yield. The secondary amine was reacted with 2,4-dichloro-5-nitropyrimidin to form **3**. The reduction of

[*] Dr. G. Budin,[+] Dr. K. S. Yang,[+] Dr. T. Reiner, Prof. R. Weissleder
Center for Systems Biology, Massachusetts General Hospital
185 Cambridge Street, Boston, MA 02114 (USA)
E-mail: rweissleder@mgh.harvard.edu
Prof. R. Weissleder
Harvard Medical School
200 Longwood Avenue, Boston, MA 02115 (USA)
[+] These authors contributed equally to this work.

[**] This work was supported by the National Institutes of Health (NIH) grant number RO1EB010011, K.S. was supported by a NIH grant T32-CA79443 and T.R. was supported by a grant from the German Academy of Sciences Leopoldina (LPDS 2009-24). We thank Joshua Dunham and Alex Zaltsman for image processing, and Dr. Robert Yang and Prof. Peter Sorger for assistance with cellWoRx and Image Rail.

Supporting information for this article is available on the WWW under http://dx.doi.org/10.1002/anie.201103273.

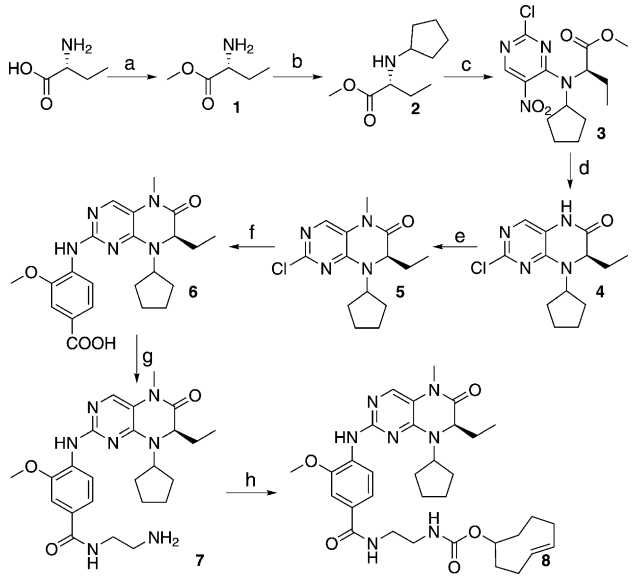

Scheme 1. Synthesis of the bioorthogonal probe BI 2536-TCO (**8**). Reagents and conditions: a) MeOH, $SOCl_2$, 0°C to reflux, 1.5 h, quant.; b) cyclopentanone, NaOAc, DCM, $HB(OAc)_3Na$, 0°C to RT 12 h, 97%; c) 2,4-dichloro-5-nitropyrimidin, K_2CO_3, acetone, 0°C, then 12 h at RT, 55%; d) 1. AcOH, 70°C, 2. Fe powder, 1 h, 70°C, 3. 1.5 h, 100°C, 44%; e) 1. MeI, DMA, NaH, −10°C, 2. 20 min, 0°C, 3. 30 min, RT, quant.; f) 4-amino-3-methoxybenzoic acid, $EtOH/H_2O$, HCl_{conc}, reflux, 48 h, 55%; g) ethylenediamine, DIPEA, BOP, DMF, 3 h, RT, 56%; h) TCO-NHS, DIPEA, DMF, 1 h, RT, 49%. DCM = dichloromethane, DMA = dimethylacetamide, DIPEA = diisopropylethylamine, BOP = (benzotriazol-1-yloxy)tris(dimethylamino)phosphonium hexafluorophosphate.

the nitro group was performed using iron and glacial acetic acid leading to an in situ intramolecular cyclization affording compound **4** in 46% yield. Methylation of the secondary amine and amination of the chloropyrimidine by 4-amino-3-methoxybenzoic acid afforded the desired compound **6**. The free carboxylic acid of compound **6** was first engaged in a peptidic coupling with an ethylene diamine spacer and the resulting free amine **7** was reacted with a *trans*-cyclooctene moiety activated by a *N*-hydroxysuccinimide ester group (TCO-NHS) affording BI 2536-TCO (**8**) in 49% yield (for detailed procedure see the Supporting Information).

The reactivity of BI 2536-TCO (**8**) and tetrazine was first investigated. The cycloaddition was realized by mixing at 0.25 mM the drug and a tetrazine compound bearing a fluorescent dye Texas Red-Tz. Texas Red was chosen for its ability to reach the nucleus (unpublished data) but other dyes that permeate into the nucleus could also be used. After stirring for two minutes, the sample was analyzed by HPLC-MS. LC-MS spectra confirmed the quantitative conversion of Texas Red-Tz to the clicked product **9** (Scheme 2 and Figure S1).

The inhibitory effect of BI 2536, BI 2536-TCO (**8**), Texas Red-Tz and the pre-reacted BI 2536-Texas Red (**9**) were evaluated using a PLK1 kinase activity assay (see Supporting Information). The IC_{50} value of BI 2536 was 4.3 nM. Analysis of BI 2536-TCO (**8**) and BI 2536-Texas Red (**9**) resulted in IC_{50} values of 9.4 nM and 103 nM, respectively (Figure 2 and Table 1). These results indicate that the TCO linker modification on **6** only minimally affects the affinity for PLK1, whereas the use of the pre-reacted fluorescent probe **9** resulted in an increase in the IC_{50} value of approximatively 11-fold. Thus, BI 2536-TCO bioorthogonal two-step labeling procedure would seem a rational strategy for imaging and quantifying PLK1 expression in intact cells.

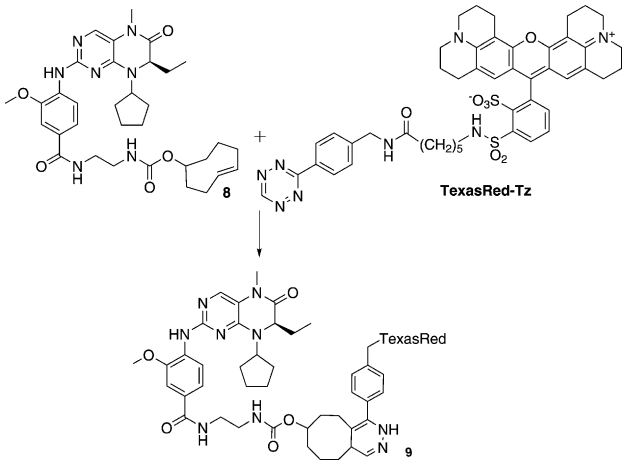

Scheme 2. Bioorthogonal reaction between BI 2536-TCO (**8**) and Texas Red-Tetrazine affording **9** (not all isomers shown).

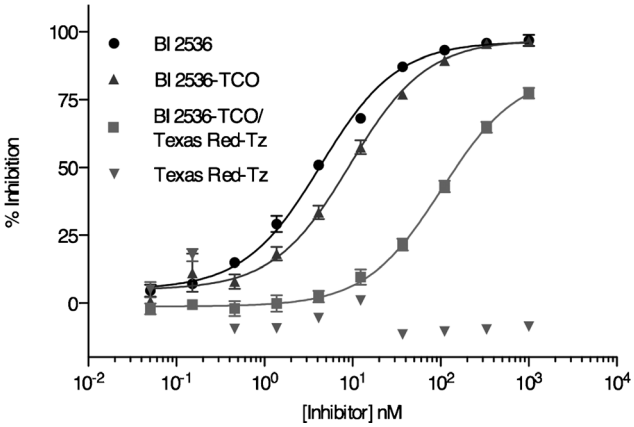

Figure 2. Inhibitory effect of BI 2536 derivatives on PLK1. The IC_{50} values for BI 2536, BI 2536-TCO, Texas Red-Tz and BI 2536-TCO pre-reacted with Texas Red-Tz were determined using the Z′-LYTE Ser/Thr-16 peptide assay kit (Invitrogen) and human recombinant PLK1. A sigmoidal dose-response was fit to data using GraphPad software (Prism).

Table 1: IC_{50} values of BI 2536 derivatives for Polo-like kinase 1.

Compound	IC_{50}	+Error	−Error
BI 2536	4.3 nM	0.71	0.61
BI 2536-TCO (**8**)	9.4 nM	2.48	1.96
BI 2536-TCO/Texas Red-Tz (**9**)	103 nM	26.58	21.13
Texas Red-Tz	≫1 μM	–	–

Colocalization between GFP-PLK1 and the bioorthogonal reaction of BI 2536-TCO (**8**) and Texas Red-Tz was investigated in PANC-1 cells. Since PLK1 is expressed during G2/M phase of the cell cycle, cells were first synchronized using a double-thymidine block, followed by a 9 h release into

normal growth media to allow cells to proceed to G2/M phase. Following synchronization, live cells were incubated for 20 min with a solution of BI 2536-TCO (**8**) in growth media (final concentration 1.5 μM, 0.1 % DMSO). Excess probe was washed out before adding Texas Red-Tz for 20 min (final concentration 1 μM, 0.1 % DMSO). Up to this step, cells were alive and were then fixed for DNA staining with Hoechst 33258 and imaging by confocal microscopy. As expected, the GFP-tagged PLK1 protein localized to kinetochores in metaphase (Figure 3 A). A strikingly similar pattern was visualized using the small molecule BI 2536-TCO (**8**) and Texas Red-Tz (Figure 3 B; note that there is predominantly nuclear staining with significantly less cytoplasmic staining, that is, along the reported distribution of PLK1[22]). Merging the images showed strong colocalization between BI 2536-Texas Red and GFP-PLK1 (Figure 3 D). Similar colocalization imaging results were obtained with HeLa cells stained with an antibody to detect endogenous PLK1 expression (Figure S2 and S3).

Control imaging experiments on cells treated either while alive or after fixing demonstrated that neither Texas Red-Tz or the pre-reacted compound **9** resulted in significant fluorescent staining, indicating the low background of the dye and the advantage of the two-step labeling procedure over a one-step procedure (Figure S2 and S3). We also observed no significant staining using unlabeled BI 2536 followed by Texas Red-Tz staining (Figure S2). Colocalization was also observed between endogenous PLK1 antibody staining and BI 2536-Texas Red during different stages of G2/M phase (Figure S3). Importantly, PLK1 antibody and BI 2536-TCO/Texas Red-Tz staining were significantly reduced in cells in interphase since PLK1 is not overexpressed during this phase. Based on these results, we are clearly able to image both GFP-PLK1 and endogenous PLK1 and recapture its appropriate localization during different phases of mitosis using BI 2536-TCO.

We next determined if BI 2536-TCO/Texas Red-Tz two-step PLK1 imaging procedure could be demonstrated in other primary cancer cell lines. We chose eight cancer cell lines (HeLa, A549, SW480, MDA-MB-231, SKOV-3, MIA PaCa-2, PANC-1, and U-87 MG) and two normal cell lines (IMR-90 and HEK-293) to compare small-molecule PLK1 imaging to the PLK1 antibody staining. Cells were plated in 96-well plates in duplicate and were treated with BI 2536-TCO and Texas Red-Tz as described above for the confocal imaging. Each well of cells was imaged at 10× magnification to examine the entire population of cells. The nuclear fluorescence intensity for the PLK1 antibody channel and separately for the Texas Red channel was determined using ImageRail software.[23] As shown in Figure 4 A, the different normal and

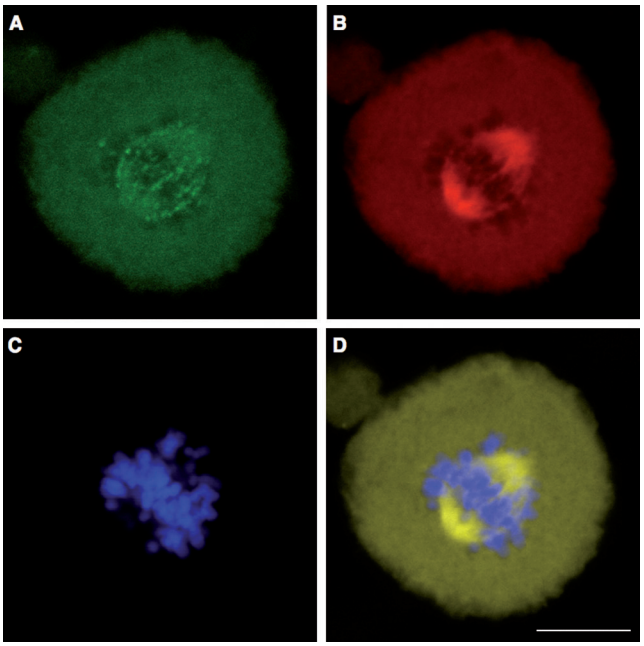

Figure 3. Colocalization of BI 2536-TCO/Texas Red-Tz with GFP-PLK1 in PANC-1 cells. Cells were synchronized at G1/S phase using a double-thymidine block, followed by a 9 h release to allow cells to proceed to G2/M phase. PANC-1 cells were then incubated for 20 min with 1.5 μM BI 2536-TCO, followed by a 20 min incubation with 1 μM Texas Red-Tz for intracellular clicking. Cells were fixed and nuclei were stained using Hoechst 33258. 60X images were collected by confocal microscopy. A) GFP-PLK1 localization in PANC-1 cells. B) BI 2536-TCO/Texas Red-Tz staining. C) Hoechst 33258 staining of PANC-1 cells. D) Merge of images (A)–(C) to show colocalization of GFP-PLK1 and BI 2536. Scale: 10 μm.

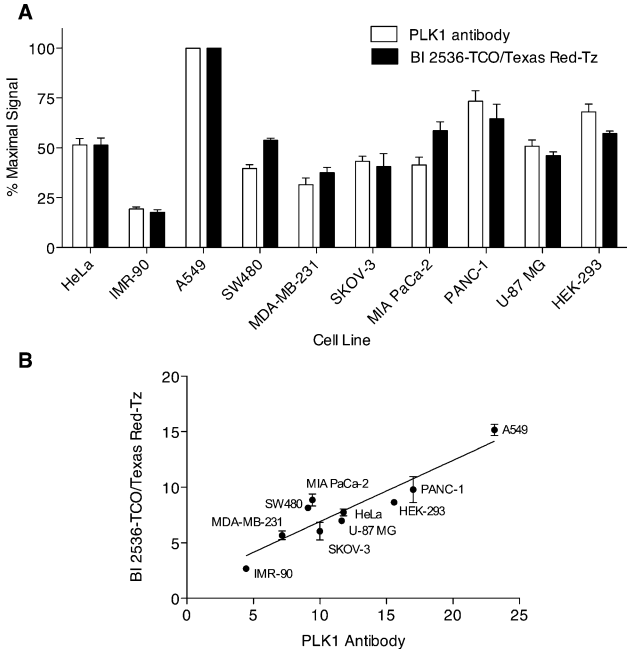

Figure 4. PLK1 expression levels were quantified using microscopy. Cell lines were plated in 96-well plates and grown for 48 h. Cells were then treated with BI 2536-TCO, followed by Texas Red-Tz. After fixing, cells were stained with an anti-PLK1 antibody and were imaged using a Cell WoRx microscope at 10× resolution (Applied Precision Instruments). A) Data were plotted as signal/background for each cell line and were normalized to the maximum value for either PLK1 antibody staining or BI 2536-TCO/Texas Red-Tz staining. B) Signal/Background data for the PLK1 antibody staining (*x*-axis) or BI 2536-TCO/Texas Red-Tz staining (*y*-axis) were plotted for each cell line and the data were fit to a straight line using GraphPad software (Prism). $R^2 = 0.843$ for the resulting linear fit. Data are presented in duplicate and are representative of at least two independent experiments. Error bars represent the unpooled sample standard error.

cancer cell lines express different levels of PLK1. These different expression levels are also reported using BI 2536-TCO/Texas Red-Tz two-step labeling with good correlation (Figure 4B, $R^2 = 0.843$).

In conclusion, we have synthesized and characterized a small-molecule PLK1 imaging agent based on BI 2536 scaffold. Using a bioorthogonal TCO/Tz approach, we were able to successfully modify BI 2536, with minimal impact on the inhibitory effect against PLK1. Imaging intact PANC-1 and HeLa cells with BI 2536-TCO/Texas Red-Tz led to striking colocalization between the probe and GFP-PLK1 or an antibody against PLK1. This colocalization was evident throughout G2/M phase of the cell cycle, suggesting the probe specifically localizes with PLK1 in the nucleus during the cell cycle. Moreover, BI 2536-TCO probe was used to quantify PLK1 expression levels in a variety of cancer cell lines of various tissue origins. Taken together, these results suggest that bioorthogonal labeling of BI 2536 is a strategy for imaging and quantifying nuclear targets. The generic method described here should have broader applications for cancer diagnosis (e.g. staining of circulating cancer cells), live cell imaging of kinases, generic imaging of targets typically considered difficult to image (e.g. nuclear targets) and scale up to whole body imaging with isotope tags. Perhaps more importantly, the described strategy could be adapted to a number of other cellular targets to visualize biological molecules, pathways and processes.

Received: May 12, 2011
Revised: July 13, 2011
Published online: August 24, 2011

Keywords: cancer · cell cycle · cycloaddition · live cell imaging · polo-like kinase

[1] D. M. Glover, I. M. Hagan, A. A. Tavares, *Genes Dev.* **1998**, *12*, 3777.
[2] E. A. Nigg, *Curr. Opin. Cell Biol.* **1998**, *10*, 776.
[3] B. C. van de Weerdt, R. H. Medema, *Cell Cycle* **2006**, *5*, 853.
[4] A. K. Roshak, E. A. Capper, C. Imburgia, J. Fornwald, G. Scott, L. A. Marshall, *Cell Signalling* **2000**, *12*, 405.
[5] F. Toyoshima-Morimoto, E. Taniguchi, E. Nishida, *EMBO Rep.* **2002**, *3*, 341.
[6] N. Watanabe, H. Arai, Y. Nishihara, M. Taniguchi, N. Watanabe, T. Hunter, H. Osada, *Proc. Natl. Acad. Sci. USA* **2004**, *101*, 4419.
[7] H. Nakajima, F. Toyoshima-Morimoto, E. Taniguchi, E. Nishida, *J. Biol. Chem.* **2003**, *278*, 25277.
[8] F. Toyoshima-Morimoto, E. Taniguchi, N. Shinya, A. Iwamatsu, E. Nishida, *Nature* **2001**, *410*, 215.
[9] M. Jackman, C. Lindon, E. A. Nigg, J. Pines, *Nat. Cell Biol.* **2003**, *5*, 143.
[10] A. E. Elia, L. C. Cantley, M. B. Yaffe, *Science* **2003**, *299*, 1228.
[11] A. E. Elia, P. Rellos, L. F. Haire, J. W. Chao, F. J. Ivins, K. Hoepker, D. Mohammad, L. C. Cantley, S. J. Smerdon, M. B. Yaffe, *Cell* **2003**, *115*, 83.
[12] A. Hanisch, A. Wehner, E. A. Nigg, H. H. Sillje, *Mol. Biol. Cell* **2006**, *17*, 448.
[13] D. M. Lowery, K. R. Clauser, M. Hjerrild, D. Lim, J. Alexander, K. Kishi, S. E. Ong, S. Gammeltoft, S. A. Carr, M. B. Yaffe, *EMBO J.* **2007**, *26*, 2262.
[14] M. R. Smith, M. L. Wilson, R. Hamanaka, D. Chase, H. Kung, D. L. Longo, D. K. Ferris, *Biochem. Biophys. Res. Commun.* **1997**, *234*, 397.
[15] F. Eckerdt, J. Yuan, K. Strebhardt, *Oncogene* **2005**, *24*, 267.
[16] J. Yuan, A. Horlin, B. Hock, H. J. Stutte, H. Rubsamen-Waigmann, K. Strebhardt, *Am. J. Pathol.* **1997**, *150*, 1165.
[17] K. Strebhardt, A. Ullrich, *Nat. Rev. Cancer* **2006**, *6*, 321.
[18] M. Steegmaier et al., *Curr. Biol.* **2007**, *17*, 316.
[19] N. K. Devaraj, S. Hilderbrand, R. Upadhyay, R. Mazitschek, R. Weissleder, *Angew. Chem.* **2010**, *122*, 2931; *Angew. Chem. Int. Ed.* **2010**, *49*, 2869.
[20] M. Kothe, D. Kohls, S. Low, R. Coli, G. R. Rennie, F. Feru, C. Kuhn, Y. H. Ding, *Chem. Biol. Drug Des.* **2007**, *70*, 540.
[21] G. Munzert, M. Steegmaier, A. Baum (Boehringer Ingelheim International GmbH), WO2006/018182A1, **2006**.
[22] L. Arnaud, J. Pines, E. A. Nigg, *Chromosoma* **1998**, *107*, 424.
[23] B. L. Millard, M. Niepel, M. P. Menden, J. L. Muhlich, P. K. Sorger, *Nat. Methods* **2011**, *8*, 487.

